Available online at www.sciencedirect.com
SCIENCE DIRECT®
Carbohydrate Polymers 53 (2003) 331–335
Carbohydrate Polymers
www.elsevier.com/locate/carbpol

Small-angle X-ray scattering studies of moderately concentrated dextran solution

Yuuki Hirata[a,*], Yoh Sano[b], Mitsuo Aoki[a], Hidekatsu Shohji[a], Shigeaki Katoh[c], Jun-ichi Abe[d], Susumu Hitsukuri[d], Hiroyuki Yamamoto[e]

[a]*Formulation Research Institute, Otsuka Pharmaceutical Factory, Inc., Kuguhara 115, Tateiwa, Muya-cho, Naruto, Tokushima, Japan*
[b]*National Food Research Institute, Kannondai 2-1-2, Tsukuba, Ibaraki, Japan*
[c]*Tokyo Research Laboratory, Meitoh Sangyo Co., Ltd, Ishikawacho 2973-2, Hachioji, Tokyo, Japan*
[d]*Faculty of Agriculture, Kagoshima University, Korimoto 1-21-24, Kagoshima, Japan*
[e]*Faculty of Textile Science and Technology, Shinshu University, Tokida 3-15-11, Ueda, Nagano, Japan*

Received 1 August 2002; revised 22 January 2003; accepted 12 February 2003

Abstract

In this study, we investigated about the molecular structure of moderately concentrated aqueous dextran solution using well-characterized dextran hydrolyzates.

The results of this study have clarified the properties of dextran molecules in aqueous solution and have confirmed the validity of small-angle X-ray scattering measurement for the investigation of dextran molecules in aqueous.

Intermolecular interactions of dextran were observed in concentrated solutions, even if the solution was not saturated. These phenomena are probably attributable to the exclusion volume effect. In addition, dextran has a core of precipitates.

Keywords: Dextran; Small-angle X-ray scattering; Exclusion volume effect

1. Introduction

Many studies have been conducted to investigate the molecular weight and degree of branching of dextran molecules, mainly employing light-scattering methods (Nakagaki & Sano, 1974).

Dextran is produced by the fermentation of sucrose by microorganisms. Partial hydrolysis and fractionation of high-molecular-weight dextran yields a product with a molecular weight in the range suitable for clinical use (Kim & Day, 1995). Moderately concentrated dextran solutions (e.g. 100 mg/ml) are usually used clinically in order to maintain physiological osmotic pressure. However, bottled dextran solutions at high concentrations are often stored for a comparatively long period of time. Inspection of stored dextran solutions sometimes reveals the presence of visible, white particulate matter. These particles are insoluble at room temperature but are soluble at higher temperature in dextran solution or water (Cadwallader, Becker, Winter, & Warcus, 1958). It is therefore important to investigate the stability of dextran solutions.

In this study, we investigated the molecular structure of moderately concentrated aqueous dextran solution using well-characterized dextran hydrolyzates.

2. Experimental section

Two samples of hydrolyzed fractionated dextran were obtained from Pharmacia Fine Chemicals (Oslo, Sweden). Table 1 shows the data supplied with the samples by the manufacturer. The weight-average molecular weight, Mw, was obtained by light scattering and the number-average molecular weight, Mn, by end-group analysis.

Small-angle X-ray scattering (SAXS) experiments using synchrotron radiation sources were carried out at room temperature with the optics and detector systems of SAXES (small-angle X-ray scattering equipment for solutions) installed on the 3.5-GeV storage ring of the Photon Factory,

* Corresponding author. Tel.: +81-886-84-2318; fax: +81-886-84-2323.
E-mail address: hiratayu@otsukakj.co.jp (Y. Hirata).

0144-8617/03/$ - see front matter © 2003 Elsevier Science Ltd. All rights reserved.
doi:10.1016/S0144-8617(03)00107-3

Table 1
Data supplied with the samples by the manufacturer

Sample	Mw	Mn	$\|\eta\|$ ml/g
Dextran T40	39,400	23,400	20
Dextran T70	66,300	36,400	26

KEK, Tsukuba, Japan. Scattering intensities were registered at 512 different angles at a wavelength (λ) of 0.149 nm in the range 0.11 $nm^{-1} < Q < 3.8\ nm^{-1}$, where Q denotes the amplitude of the scattering vector equal to $4\pi \sin \theta/\lambda$ and 2θ is the scattering angle. The SAXS experimental procedure is described in detail elsewhere (Matsumoto, Kawai, & Masuda, 1992; Ribitsch, Schurz, & Ribitsch, 1980). The SAXS intensity was measured for 600 s for all solutions and for 1200 s for buffer, and the net scattering intensities were calculated by subtracting the scattering intensities of a blank buffer solution from those of the assembly solutions (Mallm, Horkay, Hecht, Rennie, & Geissler, 1991; Veljkovic, Lazic, & Cakic, 1988). Measurements of high-molecular-weight dextran were obtained using a gel permeation chromatography-low angle light scattering system (GPC-LALLS).

3. Results and discussion

3.1. Radius of gyration of dextran

SAXS experiments of well-characterized dextran hydrolyzates, T40 and T70, were carried out over a range of concentrations from 1.25 to 100 mg/ml. The radius of gyration, Rg, is a useful parameter for assessing the size of dextran. When the logarithm of the X-ray scattering intensity at $Q, T(Q)$, is plotted against the square of Q (the so-called Guinier plot), a linear relationship is usually seen over the range $Q \cdot \mathrm{Rg} < -1$, and the slope of the line gives the value of Rg. Fig. 1 shows the concentration dependence of the Rg of T40 and T70 samples obtained with SAXS and synchrotron radiation using a Kratky camera. The synchrotron radiation source has higher intensity and

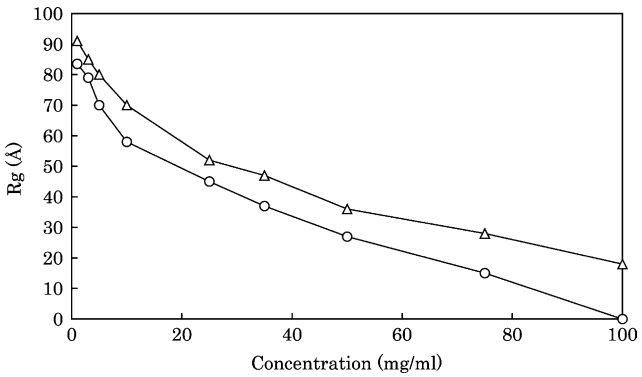

Fig. 1. Concentration dependence of Rg of T40 and T70 samples obtained with SAXS. △: T70, ○: T40.

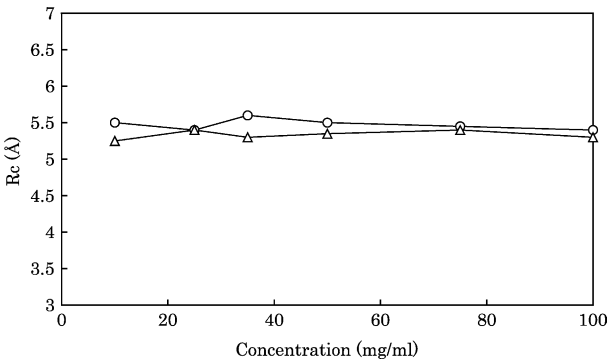

Fig. 2. Radius of the cross section, Rc, of T40 and T70. △: T40, ○ T70.

resolution than the Kratky camera, so we can precisely measure smaller angle regions, i.e. smaller Guinier regions. We checked the confidence level of the data in these regions with human serum albumin (HSA) in 0.1 M-phosphate buffer at pH 7.2, where the second virial coefficient is almost zero. The Rg for HSA was 2.8 nm, which is in good agreement with values reported in the literature (Pean et al., 1998). As shown in Fig. 1, the Rg falls sharply as the dextran concentration increases. That is to say, the intermolecular interactions of dextran molecules are dependent on the dextran concentration. This result suggests that dextran molecules in 100 mg/ml (10%) dextran solution for clinical use are closely associated.

3.2. Cross section of dextran

The radius of the cross section, Rc, was obtained. As shown in Fig. 2, the Rc did not show concentration dependence as predicted by theory and there was no appreciable difference between T40 and T70. The length of the anhydroglucose ring (i.e. one 1,4-glucosyl unit) is 0.515 nm, and one 1,6-glycosyl unit is about 0.8 nm (Garg & Stivala, 1978). Therefore, the Rc value reported in this paper corresponds to the length of a 1,4-glycosyl unit.

3.3. Molecular structure of dextran

In synthetic polymer chemistry, the Kratky plot is usually employed to evaluate the shape and the order of extension of a linear or branched-chain polymer. Even if polymers have the same Rg value in solution, Kratky plots reveal differences according to their shape and chain extension (e.g. a spherical shape yields a sharp peak, a Gaussian chain yields a horizontal line, and a rigid rod yields a straight line with a slope of 1). The Kratky plot is obtained by plotting the X-ray scattering intensity, $I(Q)$, multiplied by the square of Q against Q, and is more sensitive than the Guinier plot in revealing changes in polymer chain configuration.

Fig. 3 shows Kratky plots of dextran at 10, 50, and 100 mg/ml, indicating a typical randomly coiled structure. Dextran at order concentrations showed the same pattern.

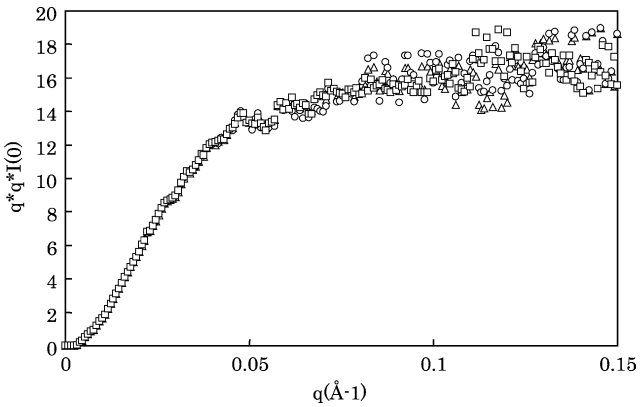

Fig. 3. Kratky plots of dextran at 10, 50, and 100 mg/ml. △: 10 mg/ml, ○: 50 mg/ml, □: 100 mg/ml.

Therefore, dextran molecules in solution behave as almost randomly coiled structures.

Dextran molecules dissolved in water and/or in physiological saline solutions are nearly ideal statistical coils and no association occurs (Basedow & Ebert, 1979). Basedow and Ebert (1979) showed that in a poor solvent such as glycerol, dextran coils are rather compact, whereas they are more expanded in a good solvent such as formamide. In dilute saline solutions, dextran coils are slightly more expanded than in water (Basedow & Ebert, 1979).

From calorimetric measurements, Basedow and Ebert (1979) reported that dextran molecules once dissolved showed no or only very little change in coil dimensions during dilution and that association-dissociation phenomena did not occur with partially hydrolyzed dextrans in dilute solutions.

The values of the relation times of water protons in dilute dextran solutions (<1%), aqueous solutions of dextran with a molecular weight range from 17×10^3 to 500×10^3, were highly sensitive to the temperature-time prehistory of the samples investigated (Fedin, Tsitsishvili, Grinberg, Bakari, & Tolstoguzov, 1975).

In concentrated solutions, Fedin et al. (1975) found that dextrans produced by various bacterial strains are strongly associated and that these aggregates are highly stable with dilution at low temperatures, but disintegrate rapidly at a temperature around 100 °C. Dextran aggregation is explicitly observed only for samples with a rather low molecular weight (less than 1×10^4). Concentrated solutions of dextrans of low molecular weight grow perceptibly turbid over time. Visual effects do not accompany aggregation of dextrans with a higher molecular weight in solution.

3.4. Distance distribution function

Another index of polymer chain conformation is the distance distribution function $P(r)$. This function is obtained by Fourier-transforming the X-ray scattering intensity function, $I(Q)$, multiplied by $Q{\cdot}r$, and represents a statistical distribution function of a pair of points separated by a distance of r nm within a polymer molecule.

3.5. Theoretical considerations

3.5.1. Properties of dextran in moderately concentrated solution

In contrast to the dilute, non-overlapping condition, dextran coils in moderately concentrated solution overlap. At the overlap threshold ($c = c^*$) the coils start to become densely packed. Based on the values of the molecular weight and the radius of gyration extrapolated to zero concentration of dextran (Table 1), the overlap threshold polymer concentration,c^*, is 23 mg/ml for dextran T40 and 29 mg/ml for dextran T70.

For a solution of neutral polymers at a semi-dilute concentration at which the chains overlap strongly but the solvent fraction is still large, the scattering intensity is given by a Lorentzian equation:

$$I(Q)/c = K/(1 + Q^2 z^{-2}) \qquad \text{for } zQ < 1,$$

where z is the static correlation length representing the range of the spatial correlation of concentration fluctuation in the system. According to scaling theory, z is independent of the molecular weight of the polymer and is expected to scale with the polymer concentration.

At shorter distances ($r < z$), the correlation is determined by the excluded volume effect. At large distances ($z < r <$ Rg), the chains are Gaussian and the effective interaction between subunits of the same chain is weak.

We next attempted to compare the experimental scattering curves with the suitable models. In the case of mixed solutes consisting of two different sizes, where each is given as a randomly coiled model, the experimental curves did not fit over the entire range of Q.

On the other hand, for distances larger than z, global conformation is observed, whereas for distances smaller than z, short-range interactions are predominant. For semi-crystallized samples, the scattering function of the Gaussian chains at the initial stage of the crystallization process, is given by the classical Debye form. At the final stage of the crystallization process the contacts of the polymer chains at the overlapping concentration become very important, which may be considered to be interchain clustering. However, the experimental curves also did not fit the theoretical curves calculated for the mixtures with both normal Gaussian chain and Gaussian clustered chains.

3.5.2. Analysis from Lorentzian and Gaussian modes

The shorter correlation length, z, was assumed to describe the rapid fluctuations in the positions of the polymer chains, while a longer distance is needed to account for the static accumulations of polymer pinned down by junction points or clusters of such points. For a neutral

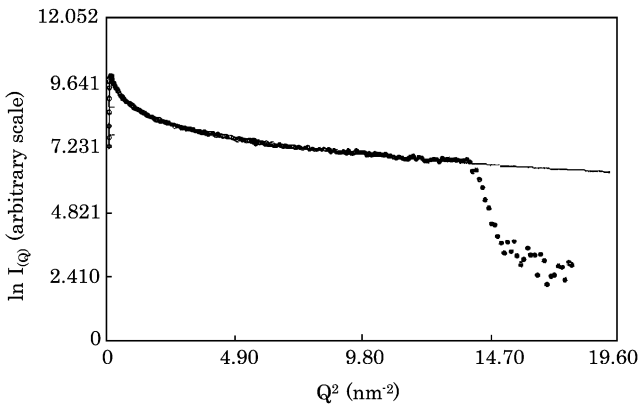

Fig. 4. Theoretical curve and experimental data of Guinier approximation (Lorentzian and Gaussian modes).

polymer solution such as dextran at equilibrium, the scattering intensity in the range $zQ \leq 1$ is described by the Lorentzian form. On the other hand, due to the variations in static concentration caused by puckering of the network by cross-links, a contribution from the regions of the sample where movement is restricted by the cross-links must also be included, and these regions have a Gaussian spatial distribution. Thus, analysis of the total scattering intensity curves was performed by a nonlinear fitting procedure to

$$I(Q) = I_L(0)/(1 + Q^2z^2) + I_G(0)\exp(-Q^2\mathrm{Rg}^{2/3}),$$

where $I_L(0)$ and $I_G(0)$ are the linear coefficients of the Lorentzian and Gaussian terms, respectively; z is the correlation length of the polymer–polymer interactions, which occur between the fluctuating chains of the homogeneous network; and Rg is the mean size of the static inhomogeneities. We assumed that these inhomogeneities arise from stationary density variations due to regions of higher polymer concentration as a result of clustering. The Gaussian term in this equation then describes the Guinier approximation for the scattering from these regions, giving their average radius of gyration.

Theoretical curves are shown in Fig. 4, with the solid line taking into account both Lorentzian and Gaussian modes.

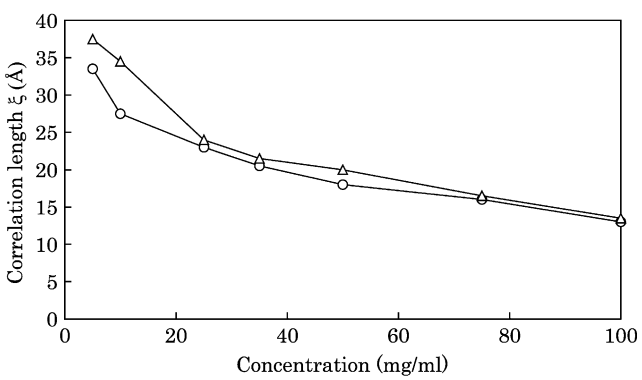

Fig. 5. Correlation length of the polymer-polymer interaction (Lorentzian and Gaussian modes). △: T70, ○: T40.

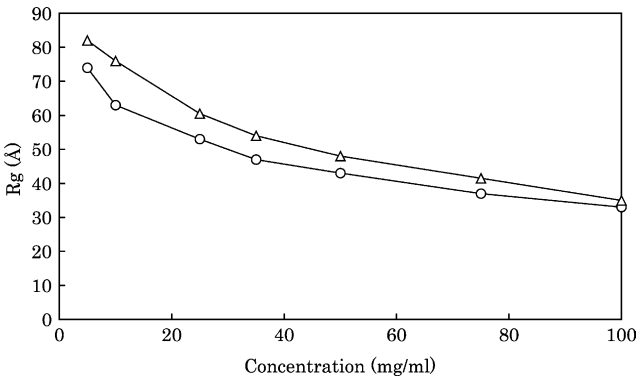

Fig. 6. Rg of dextran (Lorentzian and Gaussian modes). △: T70, ○: T40.

Experimental data showed very good agreement with the theoretical values over a wide range of Q.

The correlation length of the polymer–polymer interactions is shown in Fig. 5. The correlation length of T70 is larger than that of T40 at low concentrations, (less than 20 mg/ml). However, at high concentrations, no relationship between molecular weight and correlation length is observed. Therefore, the interactions of dextran molecules are not dependent on the molecular weight at high dextran concentrations.

The radius of gyration is shown in Fig. 6. The radius of gyration of T70 is larger than that of T40 over all concentrations. However, there are only small differences in the radius of gyration of T70 and T40. In addition, the differences in the radius of gyration increase as the dextran concentration decreases.

3.6. Structural studies of aqueous solutions of dextran and aggregated dextran

Fig. 7 shows the Rg of dextran (Mw 32,000) and aggregated dextran (containing precipitates) in aqueous solution. As shown in Fig. 7, the Rg falls sharply with an increase in dextran concentration. In addition, the Rg of aggregated dextran is smaller than that of dextran at low dextran concentrations (less than 1% w/v), while the same

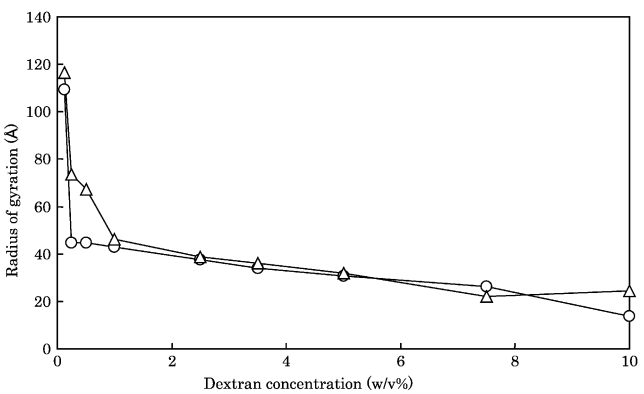

Fig. 7. Rg of dextran (Mw 32,000) and aggregated dextran (containing precipitates) in aqueous solution. △: dextran (Mw 32,000), ○: aggregated dextran (containing precipitates).

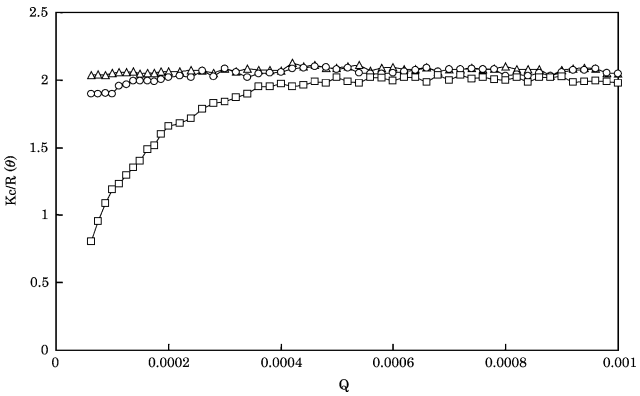

Fig. 8. Light-scattering data for aggregated dextran in aqueous solution (5% w/v). △: filtered with a 0.2 μm pore size, ○: filtered with a 0.45 μm pore size, □: filtered with a 1.2 μm pore size filter.

values are observed at high concentrations. These results suggest that a fraction of dextran molecules showing intermolecular interaction formed in aggregated dextran aqueous solution. The aggregated dextrans interact strongly with each other, and this interaction is not eliminated by dilution. The intermolecular structure is similar to that in concentrated dextran solutions (e.g. 30 mg/ml).

Fig. 8 shows the light-scattering data for aggregated dextran in aqueous solution (5% w/v). No concentration dependence was observed in the light-scattering profile of a sample filtered with a 0.2 μm pore size. In the light-scattering profile of a sample filtered with a pore size of 0.45 μm or larger, concentration dependence of the intensity of scattered light was observed, and was characteristic in low-angle regions. Therefore, particles (or intermolecular interacted structures) measuring at least 0.45 μm are present in aggregated dextran solution.

These results suggest that intermolecular interactions occur in concentrated dextran solutions, even if the solution is not saturated. These phenomena are probably attributable to the exclusion volume effect.

3.7. Measurement of the high-molecular-weight fraction in aqueous solutions of dextran

A GPC-LALLS chart of an aqueous solution of dextran is shown in Fig. 9. A leading fraction is observed in the GPC-LALLS chart. This leading peak was not reduced by heating (106 °C, 40 min). In addition, the molecular weight of this leading fraction estimated from the GPC-LALLS chart of the molecular weight standard puluran is about 6×10^6, and that of the main fraction is about 3×10^4.

These results suggest that dextran has a high-molecular-weight fraction that is clearly separated from the main fraction. Dextran has a core of precipitates, and generally,

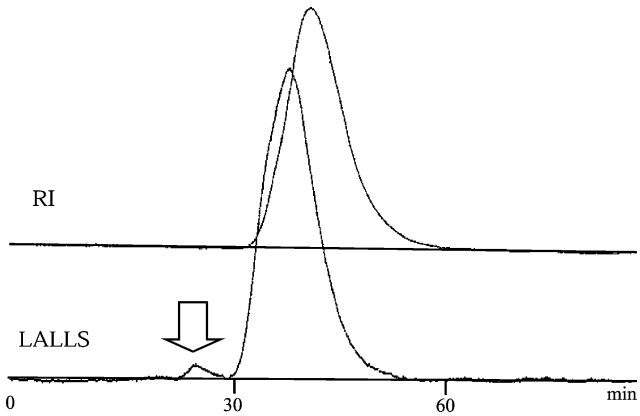

Fig. 9. GPC-LALLS chart of aqueous solution of dextran. RI: refractive index chart.

a core is an accelerator of aggregation. Therefore, dextran complex form in concentrated solutions, even if the solution is not saturated.

4. Conclusion

The properties of dextran molecules in aqueous solution have been clarified and the validity of SAXS measurement for the investigation of dextran molecules in aqueous solution has been confirmed.

Intermolecular interactions of dextran occur in concentrated solutions, even if the solution is not saturated. These phenomena are probably attributable to the exclusion volume effect. In addition, dextran has a core of precipitates.

References

Basedow, A. M., & Ebert, K. H. (1979). *Journal Polymer Science Polymer Symposium*, *66*, 101.

Cadwallader, D. E., Jr, Becker, C. H., Winter, J. H., & Warcus, D. J. (1958). *American Pharmacy Association (Science)*, *47*, 894.

Fedin, E. I., Tsitsishvili, V. G., Grinberg, V. Y., Bakari, T. I., & Tolstoguzov, V. B. (1975). *Carbohydrate Research*, *39*, 193.

Garg, S. K., & Stivala, S. S. (1978). *Journal of Polymer Science*, *16*, 1419.

Kim, D., & Day, D. F. (1995). *Letters in Applied Microbiology*, *20*(5), 268.

Mallm, A., Horkay, F., Hecht, A. M., Rennie, A. R., & Geissler, E. (1991). *Macromolecules*, *24*, 543.

Matsumoto, T., Kawai, M., & Masuda, T. (1992). *Macromolecules*, *25*, 5430.

Nakagaki, M., & Sano, Y. (1974). *Yakugaku Zasshi*, *94*(12), 1639.

Pean, J. M., Venier-Julienne, M. C., Filmon, R., Sergent, M., Phan-Tan-Luu, R., & Benoit, J. P. (1998). *International Journal of Pharmceutics*, *166*(1), 105.

Ribitsch, G., Schurz, J., & Ribitsch, V. (1980). *Colloid Polymer Scientific*, *258*, 1322.

Veljkovic, V. B., Lazic, M. L., & Cakic, M. D. (1988). *Pharmazie*, *43*, 840.